Direct numerical simulation of air-cooled and air-heated channels

Modesti, Davide; Pirozzoli, Sergio

DOI
10.1115/GT2024-122883

Publication date
2024

Document Version
Final published version

Published in
Heat Transfer

Proceedings of ASME Turbo Expo 2024: Turbomachinery Technical Conference and Exposition

(GT2024)

Volume 8

June 24-28, 2024
London, United Kingdom

Conference Sponsor
International Gas
Turbine Institute

THE AMERICAN SOCIETY OF MECHANICAL ENGINEERS

TOC

ISBN: 978-0-7918-8800-1

Proceedings of ASME Turbo Expo 2024
Turbomachinery Technical Conference and Exposition
GT2024
June 24-28, 2024, London, United Kingdom

GT2024-122883

DIRECT NUMERICAL SIMULATION OF AIR-COOLED AND AIR-HEATED CHANNELS

Davide Modesti[1,*], Sergio Pirozzoli[2],

[1]Faculty of Aerospace Engineering, Delft University of Technology, Delft, The Netherlands
[2]Dipartimento di Ingegneria Meccanica e Aerospaziale, Sapienza Universitá di Roma, Rome, Italy

ABSTRACT

We develop a theoretical framework for predicting friction and heat transfer coefficients in variable-properties forced-air convection, as typical of turbine blade cooling. To do this, we borrow concepts from high-speed wall turbulence, also featuring large temperature and density variations. Using the mean momentum balance and mean thermal balance equations we develop integral transformations that account for the effect of the variable fluid properties, and apply the inverse transformations to calculate the friction and heat transfer coefficients. The proposed theory is validated using a direct numerical simulation dataset spanning both heating and cooling conditions, and the predicted friction and heat transfer coefficients match DNS data with 1–2% accuracy.

Keywords: forced thermal convection, direct numerical simulation, variable-fluid properties, forced-air convection

NOMENCLATURE

Roman letters

$\vec{q}$	Heat flux vector [W m^{-2}]
$\vec{u}$	Velocity vector [m s^{-1}]
T	Fluid temperature [K]
C_p	Specific heat capacity at constant pressure [J kg^{-1} K]
R	Air constant [J kg^{-1} K]
h	Channel half width [m]
y	Wall distance [m]
z	Spanwise spatial coordinate [m]
ΔT	Time averaging interval [s]
u_τ	Friction velocity [m/s]
θ_τ	Friction temperature [K]

Greek letters

α	Thermal diffusivity [m^2 s^{-1}]
ν	Kinematic viscosity [m^2 s^{-1}]
μ	Dynamic viscosity [Kg m^{-1} s^{-1}]
λ	Thermal conductivity [W m^{-1} K^{-1}]
ρ	Fluid density [Kg m^{-3}]
τ	Viscous stress [Kg m^{-1}s^{-2}]
θ	Relative fluid temperature T-T_w [K]
δ_v	Viscous length scale [m]
ν_T	Eddy viscosity [m^2 s^{-1}]
α_T	Thermal diffusivity [m^2 s^{-1}]

Dimensionless groups

Re	Reynolds number
Pr	Prandtl number
St	Stanton number
Nu	Nusselt number
γ	Specific heat capacity ratio
C_f	Friction coefficient
f	Kernel function for wall distance transformation
g	Kernel function for velocity transformation
h	Kernel function for temperature transformation
R	local-to-wall mean density ratio
N	local-to-wall mean kinematic viscosity ratio
η	nondimensional wall distance
κ	Kármán constant
C_{v1}	First eddy viscosity constant
C_{v2}	Second eddy viscosity constant

Superscripts and subscripts

$+$	Viscous units
w	wall value
b	bulk value
m	mixed mean temperature value
cp	constant properties
vp	variable properties

1. INTRODUCTION

Forced thermal convection has countless applications in engineering, such as radiators, heat pumps, fuel cells, nuclear plants, and solar receivers. A notable application of forced-air convection in aerospace engineering is cooling of turbine blades in aircraft engines, where air is spilled from the compressor and

*Corresponding author: d.modesti@tudelft.nl
Documentation for `asmeconf.cls`: Version 1.36, April 7, 2024.

TABLE 1: Flow parameters for plane channel flow DNS. Box dimensions are $6\pi h \times 2h \times 2\pi h$ for all flow cases. $Re_b = 2\rho_b h u_b/\nu_m$ is the bulk Reynolds number and $Re_\tau = h u_\tau/\nu_w$ is the friction Reynolds number. $Re_{\tau,cp}$ is the equivalent friction Reynolds number, defined in equation (13). T_m and T_w and the mixed mean temperature and the wall temperature, respectively. $C_f = 2\tau_w/(\rho_b u_b^2)$ is the friction coefficient, St is the Stanton number and Nu is the Nusselt number. Δx and Δz are the mesh spacing in the streamwise and spanwise directions, and Δy_w is the mesh spacing at the wall, all normalized with the equivalent constant property viscous length scale $\delta_{v,cp}$

	Re_b	Re_τ	T_m/T_w	$T_w(K)$	$Re_{\tau,cp}$	$C_f \times 10^3$	$St \times 10^3$	Nu	N_x	N_y	N_z	Δx^*	Δy_w^*–Δy_{max}^*	Δz^*
L04	17159	154	0.4	800	531	5.43	3.12	38.6	1024	280	512	9.8	0.53–5.1	6.5
L05A	20313	212	0.5	293.15	618	5.56	3.27	47.8	1024	280	512	11.4	0.44–6.0	7.6
L05B	17097	205	0.5	800	510	5.6	3.25	40	1024	280	512	9.4	0.51–4.9	6.3
L2	7629	552	2	293.15	223	8.05	4.69	25.8	1024	280	512	4.1	0.16–2.1	2.7
L3	9275	1075	3	293.15	267	8.29	4.89	32.6	1024	280	512	4.9	0.26–2.6	3.3
H04	31756	258	0.4	800	831	4.48	2.69	61.4	2048	480	1024	7.7	0.52–4.6	5.1
H05A	37551	359	0.5	293.15	1037	4.65	2.72	73.6	2048	480	1024	9.5	0.52–5.8	6.4
H05B	37893	403	0.5	800	1004	4.46	2.62	71.4	2048	480	1024	9.2	0.63–5.6	6.2
H2	15393	1039	2	293.15	419	6.93	4.05	44.9	2048	480	1024	3.9	0.26–2.3	2.6
H3	13012	1445	3	293.15	360	7.56	4.44	41.6	2048	480	1024	3.3	0.18–2.0	2.2

pumped inside the blades to guarantee their integrity. Most studies on forced thermal convection regard the temperature field as a passive scalar, neglecting its feedback effect on the velocity field through the variation of the transport properties of the fluid. Regarding the heat transfer prediction, the effect of variable-fluid properties is accounted for using empirical corrective factor $(\mu_m/\mu_w)^n$[1] applied to to the Nusselt number resulting from formulas obtained for the constant-property case, where μ_m and μ_w are the viscosities of the fluid evaluated at the mean and wall temperatures, respectively. However, these corrections are fluid-dependent, are available only for a limited number of fluids, and their accuracy is often questionable. Although studies focusing on the effect of density and viscosity variations in forced thermal convection are available[1, 2], predictive formulas for the heat transfer and friction coefficients are invariably based on empirical fitting of experimental data, and the few numerical studies available did not discuss in detail the prediction of these coefficients. In this study, we aim to develop a more solid theoretical framework to estimate the mean friction drag and heat transfer in the presence of variation of the transport properties, limiting ourselves to the case of air as the working fluid. For that purpose, we use direct numerical simulation (DNS) data of plane turbulent channel flow at a moderate Reynolds number to evaluate the most common formulas used in engineering and develop improvements.

2. METHODOLOGY

We solve the compressible Navier–Stokes equations using our flow solver STREAmS [3, 4]. The equations are discretized using a sixth-order energy-conserving scheme for the nonlinear terms and a second-order central scheme for the viscous terms. A third-order Runge–Kutta scheme is used for time advancement. A detailed description of the numerical method is available in the reference publication [3] and STREAmS solver is available open source on Github. The streamwise momentum equation is forced in such a way as to maintain a constant mass flow rate. Periodicity is exploited in the streamwise and spanwise directions, and isothermal no-slip boundary conditions are used at the channel walls. Let h be the half-width of the channel, the DNS have been carried out in a computational domain $L_x \times L_y \times L_z = 6\pi h \times 2h \times 2\pi h$. A uniform bulk cooling or heating term is added to the energy equation to guarantee that the mixed mean temperature, defined as,

$$T_m = \frac{1}{2h\rho_b u_b}\int_0^{2h} \overline{\rho}\,\overline{\tilde{u}}\overline{T}\,\mathrm{d}y, \quad \rho_b = \frac{1}{2h}\int_0^{2h}\overline{\rho}\,\mathrm{d}y, \quad u_b = \frac{1}{2h\rho_b}\int_0^{2h}\overline{\rho}\,\overline{\tilde{u}}\,\mathrm{d}y, \quad (1)$$

remains exactly constant in time. Here, ρ_b and u_b are the bulk density and velocity, respectively. This forcing method corresponds to adding uniform bulk heating to balance heat losses, however, other forcing strategies are possible [e.g. 5, 6]. The most common alternative to uniform bulk heating is enforcement of constant heat flux in time. Both approaches have advantages and disadvantages. Uniform bulk heating is less realistic as it is difficult to attain in experiments [5], however it is more efficient from a computational point of view because of faster convergence towards a statistically stationary state. In the present work we opt for uniform bulk heating in light of higher computational efficiency in DNS of high-Reynolds-number flows. We also note that while the effect of different forcing methods has been studied extensively in the context of passive scalars, and it is considered to be small, we are not aware of any similar study for variable property fluids.

In the following, the overline symbol is used to indicate Reynolds averaging in time and in the homogeneous spatial directions, and the prime superscript is used to denote fluctuations with respect to the Reynolds average. All flow cases have been averaged in time for about $30\Delta T h/u_\tau$. As common in variable-density flows, we also use Favre averages, denoted with the tilde superscript $\tilde{f} = \overline{\rho f}/\overline{\rho}$, and the double prime superscript will indicate fluctuations with respect to $\tilde{f}$.

The + superscript is used to denote wall units, namely quantities made nondimensional with respect to the friction velocity, $u_\tau = (\tau_w/\overline{\rho}_w)^{1/2}$ (where $\tau_w = \mu_w d\overline{\tilde{u}}/dy|_w$ is the mean wall shear stress), and the associated viscous length scale, $\delta_v = \nu_w/u_\tau$, where the subscript 'w' denotes quantities evaluated at the wall.

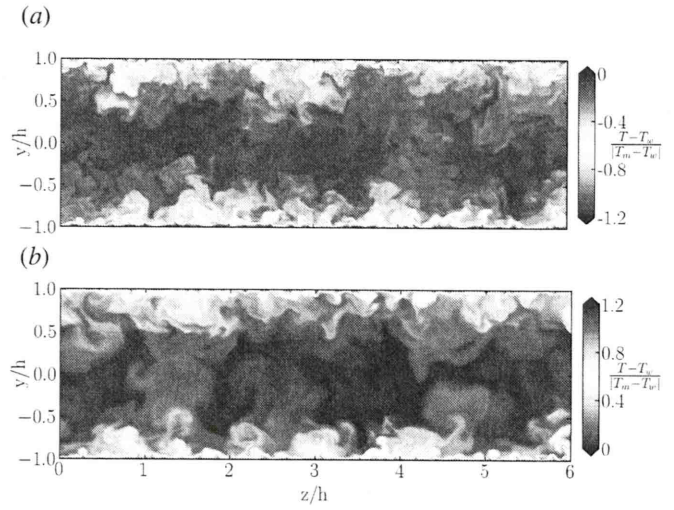

FIGURE 1: Instantaneous temperature field in a cross-stream plane, for flow case H05A (T_m/T_w = 0.5, Re_b = 37551, Re_τ = 403) (*a*) and H3 (T_m/T_w = 3, Re_b = 12012, Re_τ = 1445) (*b*).

For inner normalization of the mean temperature, we use the friction temperature, $\theta_\tau = q_w/(\rho_w c_p u_\tau)$, where $q_w = \lambda_w d\widetilde{T}/dy|_w$ is the mean wall heat flux, where $c_p = \gamma/(\gamma-1)R$ is the specific heat capacity at constant pressure, R the air constant, and λ_w is the thermal conductivity at the wall, evaluated as $\lambda = \mu c_p/Pr = 0.72$, with Prandtl number set to $Pr = 0.72$.

Ten DNS have been carried out at bulk Mach number $M_b = u_b/c_m = 0.2$ (where c_m is the speed of sound at the mixed mean temperature), and bulk Reynolds number $Re_b = 2\rho_b u_b h/\mu_m \approx 7600$–$37000$ (table 1), where μ_m is the dynamic viscosity evaluated at the mixed mean temperature. The viscosity dependence on temperature is accounted for using Sutherland's law. We consider various mean-to-wall temperature ratios, namely $T_m/T_w = [0.4, 0.5, 2, 3]$, resulting in friction Reynolds numbers in the range $Re_\tau = u_\tau h/\nu_w \approx 200$–$1000$, where ν_w is the kinematic viscosity at the wall. For a mean-to-wall temperature ratio $T_m/T_w = 0.5$, we also study the effect of the wall temperature, considering cases with $T_w = 800K$ and $T_w = 293.15K$. For each value of the mean-to-wall temperature ratio, we consider two flow cases denoted with the letter L or H, depending on whether the Reynolds number is comparatively 'low' or 'high'.

3. INSTANTANEOUS TEMPERATURE FIELD

We begin our analysis by inspecting the instantaneous temperature fields of flow cases H05 (T_m/T_w = 0.5, Re_b = 37551, Re_τ = 403) and H3 (T_m/T_w = 3, Re_b = 12012, Re_τ = 1445) in figure 1. Both cases exhibit the qualitative features that characterize wall turbulence, with cold (or hot) flow structures protruding towards the walls, and hot (or cold) fluid regions protruding towards the channel center. Despite sharing the general features of wall turbulence, we also note a significant effect of the thermodynamic and fluid property variations between wall heating and wall cooling. First, we observe that the friction Reynolds number values reported in table 1 are not indicative of actual separation of scales as in constant-property flows, and in fact flow case H05 has lower friction Reynolds number while exhibiting finer eddies. This effect can be traced to strong viscosity variations within the wall and bulk flow regions, and it is further discussed in section 4. The cooled flow case H3 indeed appears to be a 'filtered' version of the heated case, in which only the larger structures survive. In fact, in flow case H3 we observe large structures extending from one wall to beyond the channel centreline, whereas those are masked by smaller eddies in flow case H05.

4. MEAN FLOW FIELD AND VARIABLE-PROPERTIES TRANSFORMATIONS

We begin the mean flow analysis by comparing the mean velocity and temperature profiles to the equivalent statistics for the constant property case. We use synthetic profiles for the reference, constant property case. The composite profiles are obtained by matching inner layer velocity and temperature profiles with the corresponding outer layer distributions. The inner layer profiles are obtained by integrating the eddy viscosity of Musker [7] for the velocity and the eddy diffusivity proposed by Pirozzoli [8] for the temperature profile. In the outer layer we use Clauser's hypothesis of uniform eddy viscosity [9] and uniform eddy diffusivity [10]. A thorough derivation of the composite profiles is available [11].

The reference constant properties case is the composite profile proposed by Pirozzoli [8]. Figure 2 shows that the statistics of the variable-properties DNS are substantially different from the constant-properties case when scaled in classical wall units. All the flow cases exhibit deviations from the reference, starting from the buffer region, and becoming more evident in the logarithmic region, where both the logarithmic slope and the additive constant deviate from the constant-property references. In order to account for variable-properties effect, we consider the streamwise mean momentum balance equation,

$$\overline{\mu}\frac{\mathrm{d}\widetilde{u}}{\mathrm{d}y} - \overline{\rho}\widetilde{u''v''} = \overline{\rho}_w u_\tau^2 (1-\eta), \tag{2}$$

where $\eta = y/h$. Moreover, we compare equation (2) with its constant properties counterpart,

$$\mu_w\frac{\mathrm{d}\overline{u}}{\mathrm{d}y} - \rho_w\overline{u'v'} = \rho_w u_\tau^2 (1-\eta), \tag{3}$$

For similarity with the case of compressible flows, we assume that the effects of density and viscosity variations can be accounted for using suitable convolution integrals [12],

$$y_{cp} = \int_0^y f_{cp}\,\mathrm{d}y, \quad u_{cp} = \int_0^{\tilde{u}} g_{cp}\,\mathrm{d}\tilde{u}, \quad \theta_{cp} = \int_0^{\tilde{\theta}} h_{cp}\,\mathrm{d}\tilde{\theta}, \tag{4}$$

with kernel functions f_{cp}, g_{cp}, h_{cp} are to be specified such that the flow properties are mapped to the universal, constant-property case, denoted with the 'cp' subscript. Following Hasan *et al.* [13], we then introduce an eddy viscosity for the turbulent shear stress, such that $-\overline{\rho}\widetilde{u''v''} = \overline{\rho}\nu_T \mathrm{d}\tilde{u}/\mathrm{d}y$ and substitute the transformations (4) into the streamwise mean momentum balance equation. With these substitutions, equation (2) can be recast as

$$\frac{\overline{\mu}}{\mu_w}\frac{f_{cp}}{g_{cp}}\left(1+\frac{\nu_T}{\nu}\right)\frac{\mathrm{d}u^+_{cp}}{\mathrm{d}y^+_{cp}} = 1-\eta. \tag{5}$$

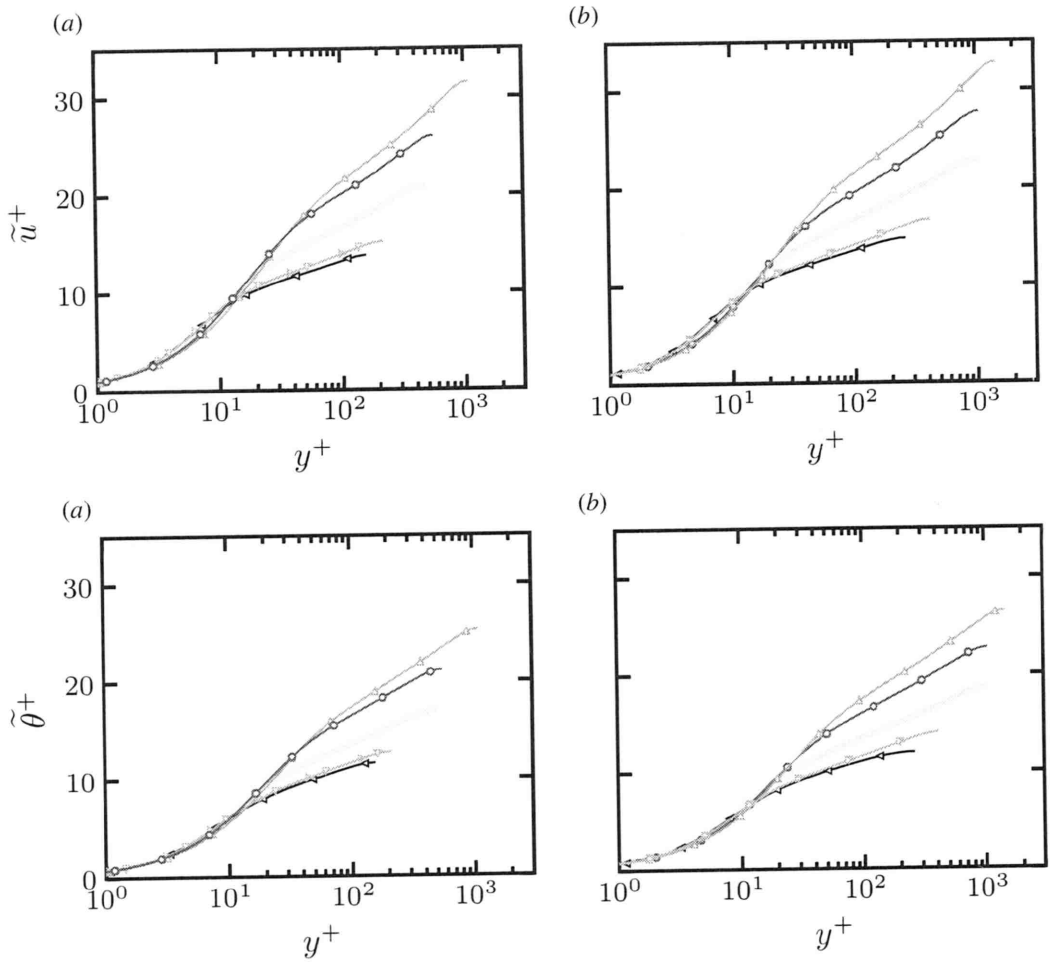

FIGURE 2: Mean velocity (*a*,*b*) and mean temperature (*c*,*d*) profiles for L flow cases (*a*,*c*) and H flow cases (*b*,*d*). Symbols indicate DNS data for different mean-to-wall temperature ratios: $T_m/T_w = 0.4, T_w = 800K$, $T_m/T_w = 0.5, T_w = 800K$ (downward triangle), $T_m/T_w = 0.5, T_w = 273.25K$ (right triangles), $T_m/T_w = 2$ (circles), $T_m/T_w = 3$ (upward triangles). Gray solid lines indicate the mean velocity and temperature profiles of the constant properties case, obtained using the synthetic velocity profile of Musker [7] and the synthetic temperature profile of Pirozzoli [8].

Comparing equation (5) with the constant-properties counterpart,

$$\left(1 + \frac{\nu_{T,cp}}{\nu}\right) \frac{\mathrm{d}u^+_{cp}}{\mathrm{d}y^+_{cp}} = (1 - \eta)\,, \tag{6}$$

and assuming that the kernel function f_{cp} is the same as in [14], we can also determine g_{cp},

$$\begin{aligned} f_{cp} &= \frac{\mathrm{d}}{\mathrm{d}y}\left(\frac{y}{R^{1/2}N}\right), \\ g_{cp} &= \left(\frac{1 + \nu_T/\nu}{1 + \nu_{T,cp}/\nu}\right) RN \frac{\mathrm{d}}{\mathrm{d}y}\left(\frac{y}{R^{1/2}N}\right), \end{aligned} \tag{7}$$

where $N = \overline{\nu}/\nu_w$, $R = \overline{\rho}/\overline{\rho}_w$.

The eddy viscosity for the constant-properties case is modeled after Musker [7], and we extend the model to account for variable properties by including an ad-hoc correction depending on the mean-to-wall temperature ratio

$$\frac{\nu_{T,cp}}{\nu} = \frac{\left(\kappa y^+_{cp}\right)^3}{\left(\kappa y^+_{cp}\right)^2 + C^2_{v1}}, \tag{8}$$

$$\frac{\nu_T}{\nu} = \frac{\left(\kappa y^+_{cp}\right)^3}{\left(\kappa y^+_{cp}\right)^2 + C^2_{v1} + \left[C_{v2}\left(1 - T_m/T_w\right)\right]^2}, \tag{9}$$

where $\kappa = 0.387$ is the assumed Kármán constant, and the constants $C_{v1} = 7.57$, $C_{v2} = 0.8$, are inferred from analysis of the DNS data. Following the same procedure used for the mean momentum equation, we then determine the kernel function for the temperature transformation,

$$h_{cp} = \left(\frac{1 + \alpha_T/\alpha}{1 + \alpha_{T,cp}/\alpha}\right) \frac{(1 - \eta)}{(1 - \mathcal{R})} RN \frac{\mathrm{d}}{\mathrm{d}y}\left(\frac{y}{R^{1/2}N}\right), \tag{10}$$

where

$$\mathcal{R}(\eta) = \frac{1}{\rho_b} \int_0^\eta \overline{\rho}(\eta)\, \mathrm{d}\eta \tag{11}$$

and $\alpha = \lambda/(\rho c_p)$ is the thermal diffusivity coefficient.

Following Pirozzoli [8], the turbulent diffusivities are modelled using the same functional of the turbulent viscosity (9).

In figure 3, we plot the transformed mean velocity and temperature profiles using the kernel functions (7) and (10), and compare the results with the reference constant properties case. The collapse of the various distributions is quite remarkable, given the wide range of variation of the flow properties which we are considering. These transformations allows us to define an equivalent channel height h_{cp}, which we use to introduce an equivalent constant-properties friction Reynolds number,

$$Re_{\tau,cp} = \frac{h_{cp}}{\delta_v}, \quad h_{cp} = \int_0^h f_{cp} \mathrm{d}y. \tag{12}$$

The equivalent channel height h_{cp} is larger than h for heating and smaller for cooling, leading to a higher or lower equivalent constant-properties friction Reynolds number. We can also define the constant-properties friction Reynolds number, using an equivalent friction velocity, which allows us to introduce constant-properties viscous units,

$$Re_{\tau,cp} = \frac{u_{\tau,cp} h}{\overline{\nu}_w}, \quad u_{\tau,cp} = \frac{\overline{\nu}_w}{\delta_{v,cp}}, \quad \delta_{v,cp} = \frac{h}{h_{cp}} \delta_v \tag{13}$$

Values of the equivalent constant-properties Reynolds numbers are reported in table 1, and allows us to better interpret the instantaneous flow field in figure 1 where flow cases with heating show finer eddies than for cooling because their effective Reynolds number is higher.

5. HEAT TRANSFER AND WALL FRICTION

The variable-properties transformations developed in the previous section are very useful especially as they enable the prediction of the heat transfer and friction coefficients. For that purpose, the only required inputs are the constant-property mean velocity and mean temperature profiles, which we take from Musker [7] and Pirozzoli [8], respectively. Starting from those, application of the inverse of transformations (4) allows us to determine the variable-properties profiles, for any given mean-to-wall temperature ratio and Reynolds number. The key technical difficulty is that the kernel functions f_{cp}, g_{cp}, h_{cp} depend on the actual temperature in the variable-property case, hence an iterative procedure must be used, similar to the one used for compressible flows [15, 16].

Figure 4 shows the resulting friction coefficient $C_f = 2\tau_w/(\rho_b u_b^2)$, and the inverse of the Stanton number $St = q_w/[\rho_b C_p u_b (T_w - T_m)]$. We find significant deviations in cases with properties variations, compared to the baseline case. In particular, we note that cases with cooled wall yield reduced friction and heat flux, whereas cases with heated wall yield an increase of momentum and heat transfer, with a scatter around the constant-properties case of ±25% for the friction coefficient, and the Stanton number. Theoretical predictions relying on use of the variable-properties transformations (4) are reported with solid line of matching colors, and of course those are no longer universal. Notably, figure 4 shows that the resulting predictions match the DNS data to within 1-2% accuracy for all cases, both for the friction and heat transfer coefficients. It is worth noting that, in the context of compressible flows, [15] found an error up to 8% on the friction and heat trnasfer coefficients. This larger uncertainty can be probably traced back to the different kernel functions they used and also to the fact that in the case of compressible flows the iterative procedure is more complex due to the temperature–velocity relation.

6. CONCLUSION

Currently, the prediction of heat transfer by forced convection in real fluids relies heavily on fitting experimental data, with resulting uncertainties up to 20-30%. In contrast, we develop a more solid framework for computing these coefficients, that is based on the underlying mean flow equations, as routinely done in high-speed turbulent boundary layers. The advantage of having a theory based on first principles is that it is generalizable and more accurate than data fitting. The results demonstrate that the method can predict heat transfer and friction coefficients with an accuracy within 1-2% compared to DNS data. Additionally, the approach also returns the mean temperature and velocity profiles, which can serve as wall functions in wall-modelled simulations. In this work we assumed constant Prandtl number and heat capacities, however, this might not be valid for large temperature variations and this effect will be explored in the future. This study has focused on the important case of air, and in the future we will also extend the theory to other working fluids. Another point of attention is the choice of the thermal forcing in the simulations. While the effect of different forcing strategies has extensively been addressed in the context of passive scalars, we are not aware of any similar studies in for variable properties flows. However, even if the thermal forcing is found to have an effect on the friction and heat transfer coefficients, this can be easily accounted for in the general strategy proposed here, only resulting in a different form of equation (11).

ACKNOWLEDGMENTS

We acknowledge CHRONOS for awarding us access to Piz Daint, at the Swiss National Supercomputing Centre (CSCS), Switzerland. We also acknowledge EuroHPC for access to LEONARDO based at CINECA, Casalecchio di Reno, Italy.

REFERENCES

[1] Yeh, F.C. and Stepka, F.S. "Review and status of heat-transfer technology for internal passages of air-cooled turbine blades." NASA Technical Paper 2232. NASA. 1984.

[2] Patel, A., Boersma, B.J. and Pecnik, R. "Scalar statistics in variable property turbulent channel flows." *Phys. Rev. Fluids* Vol. 2 No. 8 (2017): p. 084604.

[3] Bernardini, M., Modesti, D., Salvadore, F. and Pirozzoli, S. "STREAmS: A high-fidelity accelerated solver for direct numerical simulation of compressible turbulent flows." *Comput. Phys. Commun.* Vol. 263 (2021): p. 107906.

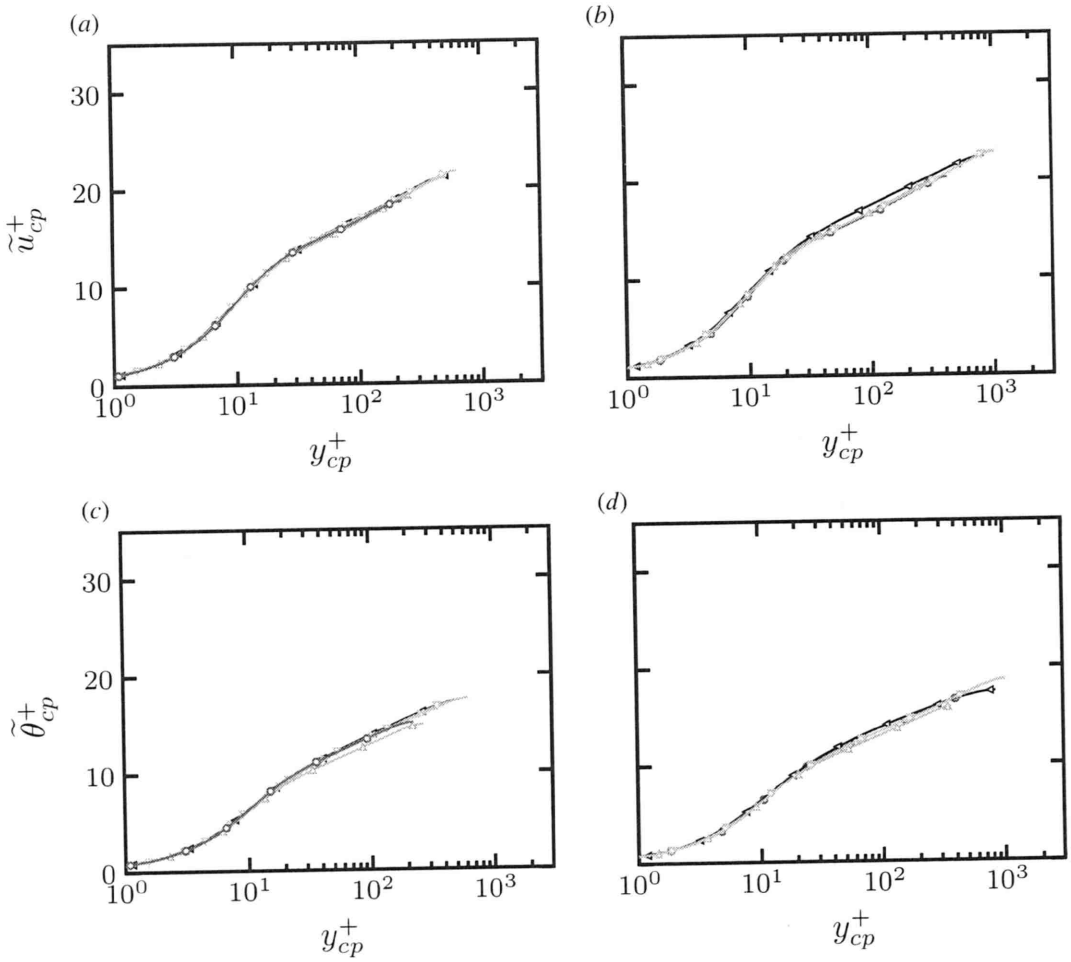

FIGURE 3: Mean velocity (*a*,*b*) and mean temperature (*c*,*d*) profiles transformed using equation (4) with kernel functions (7) and (10), for L flow cases (*a*,*c*) and H flow cases (*b*,*d*). Symbols indicate DNS data for different mean-to-wall temperature ratios: $T_m/T_w = 0.4, T_w = 800K$, $T_m/T_w = 0.5, T_w = 800K$ (downward triangle), $T_m/T_w = 0.5, T_w = 273.25K$ (right triangles), $T_m/T_w = 2$ (circles), $T_m/T_w = 3$ (upward triangles). Gray solid lines indicate the reference mean velocity and temperature profiles of the constant properties case, obtained using the synthetic velocity profile of Musker [7] and the synthetic temperature profile of Pirozzoli [8].

[4] Bernardini, M., Modesti, D., Salvadore, F., Sathyanarayana, S., Posta, G. Della and Pirozzoli, S. "STREAmS-2.0: Supersonic turbulent accelerated Navier–Stokes solver version 2.0." *Comput. Phys. Commun.* Vol. 285 (2023): p. 108644.

[5] Piller, M. "Direct numerical simulation of turbulent forced convection in a pipe." *Int. J. Numer. Methods Fluids* Vol. 49 No. 6 (2005): pp. 583–602.

[6] Abe, H. and Antonia, R.A. "Relationship between the heat transfer law and the scalar dissipation function in a turbulent channel flow." *J. Fluid Mech.* Vol. 830 (2017): pp. 300–325.

[7] Musker, A.J. "Explicit expression for the smooth wall velocity distribution in a turbulent boundary layer." *AIAA J.* Vol. 17 No. 6 (1979): pp. 655–657.

[8] Pirozzoli, S. "An explicit representation for mean profiles and fluxes in forced passive scalar convection." *J. Fluid Mech.* Vol. 968 (2023): p. R1.

[9] Pirozzoli, S. "Revisiting the mixing-length hypothesis in the outer part of turbulent wall layers: mean flow and wall friction." *J. Fluid Mech.* Vol. 745 (2014): pp. 378–397.

[10] Pirozzoli, S., Bernardini, M. and Orlandi, P. "Passive scalars in turbulent channel flow at high Reynolds number." *J. Fluid Mech.* Vol. 788 (2016): pp. 614–639.

[11] Pirozzoli, S. and Modesti, D. "Mean temperature and concentration profiles in turbulent internal flows." *Int. J. Heat Fluid Flow (Under review)* Vol. - (2024): pp. –.

[12] Modesti, D. and Pirozzoli, S. "Reynolds and Mach number effects in compressible turbulent channel flow." *Int. J. Heat Fluid Flow* Vol. 59 (2016): pp. 33–49.

[13] Hasan, A.M., Larsson, J., Pirozzoli, S. and Pecnik, R. "Incorporating intrinsic compressibility effects in velocity transformations for wall-bounded turbulent flows." *Phys. Rev. Fluids* Vol. 8 (2023): p. L112601.

[14] Trettel, A. and Larsson, J. "Mean velocity scaling for compressible wall turbulence with heat transfer." *Phys. Fluids (1994-present)* Vol. 28 No. 2 (2016): p. 026102.

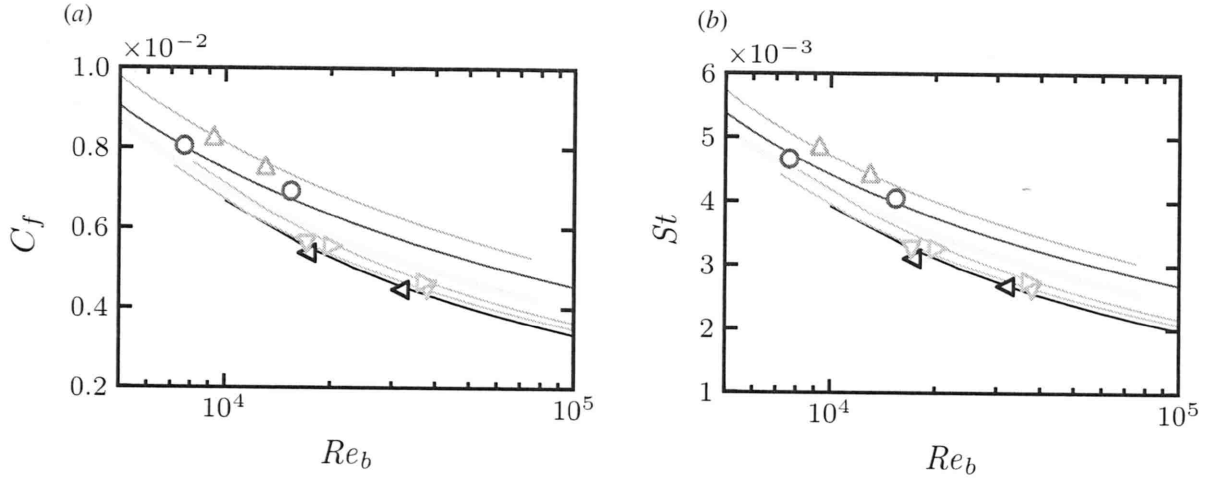

FIGURE 4: Friction coefficient (*a*), Stanton number (*b*), as a function of the bulk Reynolds number $Re_b = 2h\rho_b u_b/\mu_m$. Solid lines indicate predictions obtained inverting the present variable properties transformations, and symbols indicate DNS data for different mean-to-wall temperature ratios: $T_m/T_w = 0.4, T_w = 800K$, $T_m/T_w = 0.5, T_w = 800K$ (downward triangle), $T_m/T_w = 0.5, T_w = 273.25K$ (right triangles), $T_m/T_w = 2$ (circles), $T_m/T_w = 3$ (upward triangles).

[15] Kumar, V. and Larsson, J. "Modular method for estimation of velocity and temperature profiles in high-speed boundary layers." *AIAA J.* Vol. 60 No. 9 (2022): pp. 5165–5172.

[16] Hasan, A.M., Larsson, J., Pirozzoli, S. and Pecnik, R. "Estimating Mean Profiles and Fluxes in High-Speed Turbulent Boundary Layers Using Inner/Outer-Layer Scalings." *AIAA J.* (2023): pp. 1–6.